



Activation of two types of Ca²⁺-permeable nonselective cation channel by endothelin-1 in A7r5 cells

¹Yasushi Iwamuro, ^{2,4}Soichi Miwa, ¹Tetsuya Minowa, ³Taijiro Enoki, ²Xiao-Feng Zhang, ¹Masatsune Ishikawa, ¹Nobuo Hashimoto & ²Tomoh Masaki

Department of ¹Neurosurgery, ²Pharmacology and ³Anesthesiology, Kyoto University Faculty of Medicine, Kyoto 606-8501, Japan

1 In A7r5 cells loaded with the Ca²⁺ indicator fura-2, we examined the effect of a Ca²⁺ channel blocker SK&F 96365 on increases in intracellular free Ca²⁺ concentrations ([Ca²⁺]_i) and Mn²⁺ quenching of fura-2 fluorescence by endothelin-1 (ET-1). Whole-cell patch-clamp was also performed.

2 Higher concentrations (≥10 nM) of ET-1 (higher [ET-1]) evoked a transient peak and a subsequent sustained elevation in [Ca²⁺]_i: removal of extracellular Ca²⁺ abolished only the latter. A blocker of L-type voltage-operated Ca²⁺ channel (VOC) nifedipine at 1 μM reduced the sustained phase to about 50%, which was partially sensitive to SK&F 96365 (30 μM).

3 Lower [ET-1] (≤1 nM) evoked only a sustained elevation in [Ca²⁺]_i which depends on extracellular Ca²⁺. The elevation was partly sensitive to nifedipine but not SK&F 96365.

4 In the presence of 1 μM nifedipine, higher [ET-1] increased the rate of Mn²⁺ quenching but lower [ET-1] had little effect.

5 In whole-cell recordings, both lower and higher [ET-1] induced inward currents at a holding potential of –60 mV with linear I-V relationships and reversal potentials close to 0 mV. The current at lower [ET-1] was resistant to SK&F 96365 but was abolished by replacement of Ca²⁺ in the bath solution with Mn²⁺. The current at higher [ET-1] was abolished by the replacement plus SK&F 96365.

6 In a bath solution containing only Ca²⁺ as a movable cation, ET-1 evoked currents: the current at lower [ET-1] was sensitive to Mn²⁺, whereas that at higher [ET-1] was partly sensitive to SK&F 96365.

7 These results indicate that in addition to VOC, ET-1 activates two types of Ca²⁺-permeable nonselective cation channel depending on its concentrations which differ in terms of sensitivity to SK&F 96365 and permeability to Mn²⁺.

Keywords: Endothelin-1; nonselective cation channel; calcium; SK&F 96365; manganese, A7r5 cell

Introduction

Endothelin-1 (ET-1) is a potent vasoconstricting peptide with a long duration of action (Yanagisawa *et al.*, 1988). ET-1 binds to receptors on vascular smooth muscle cells and subsequently induces an increase in the intracellular free Ca²⁺ concentrations ([Ca²⁺]_i), which is a trigger for contraction of cells. Several mechanisms have been proposed for the elevation of [Ca²⁺]_i: (1) release of intracellularly stored Ca²⁺ via increased formation of inositol trisphosphates (IP₃) (Kasuya *et al.*, 1989; Van Renterghem *et al.*, 1988); (2) activation of voltage-operated Ca²⁺ channel (VOC) (Goto *et al.*, 1989; Inoue *et al.*, 1990) and (3) activation of other types of Ca²⁺ entry channels represented by voltage-independent Ca²⁺ channels (Enoki *et al.*, 1995b; Fasolato *et al.*, 1994; Felder *et al.*, 1994; Huang *et al.*, 1990; Minowa *et al.*, 1997; Simpson *et al.*, 1990).

Although not firmly established, the voltage-independent Ca²⁺ channels are usually classified according to the mode of activation into four groups (Clementi & Meldolesi, 1996): receptor-operated Ca²⁺ channels (Benham & Tsien, 1987), G-protein-operated Ca²⁺ channels (Komori & Bolton, 1990), store-operated Ca²⁺ channels (SOCC) (Hoth & Penner, 1992) and second messenger-operated Ca²⁺ channels (Matthews *et al.*, 1989).

SK&F 96365 was initially introduced as a blocker of receptor-mediated Ca²⁺ influx in a broad sense (Merritt *et al.*, 1990). The data are now accumulating which indicate that this drug blocks Ca²⁺ influx through some of the voltage-independent Ca²⁺ channels. So far the effects of SK&F

96365 have been examined in only a limited number of cell types and in all these cells, the drug has been found to block some of the voltage-independent Ca²⁺ channels (Chung *et al.*, 1994; Franzius *et al.*, 1994; Koch *et al.*, 1994; Wayman *et al.*, 1996). Thus Ca²⁺ channels which are resistant to this drug have not yet been reported.

It is known that Ca²⁺ signaling mechanisms in response to ET-1 are different depending on its concentrations. Namely, higher concentrations of ET-1 stimulates both release of Ca²⁺ from intracellular stores (via increased formation of IP₃) (Kasuya *et al.*, 1989; Rubanyi & Polokoff, 1994) and entry of extracellular Ca²⁺, whereas lower concentrations of ET-1 stimulates only entry of extracellular Ca²⁺ without release of Ca²⁺ from intracellular stores (Enoki *et al.*, 1995b). Thus it is possible that different Ca²⁺ entry channels are involved in the elevations of [Ca²⁺]_i induced by lower and higher concentrations of ET-1. To verify this possibility, we tested the effect of pharmacological manipulations including SK&F 96365 on the elevation of [Ca²⁺]_i and whole-cell currents in A7r5 cells (a cell line derived from rat aorta) induced by lower and higher concentrations of ET-1.

Materials

Cell culture

A7r5 cells derived from rat aortic smooth muscle cells were cultured in monolayer in Dulbecco's modified Eagle's medium

⁴ Author for correspondence.

supplemented with 10% fetal bovine serum (Hyclone) at 37°C in a humidified 5% CO₂/95% air atmosphere.

Measurement of [Ca²⁺]_i in A7r5 cells

[Ca²⁺]_i was measured using a fluorescent probe fura-2 as described (Groschner *et al.*, 1994; Minowa *et al.*, 1997). For loading of fura-2, the cultured A7r5 cells were incubated in Ca²⁺-free Krebs-HEPES solution containing 5 μM fura-2/AM (acetoxymethyl ester) for 45 min at 37°C. After centrifugation, the cells were resuspended at a density of approximately 1.25 × 10⁶ cells ml⁻¹ in Ca²⁺-free Krebs-HEPES solution containing (mM): NaCl 140, KCl 3, MgCl₂ 1, glucose 11 and HEPES 10; pH 7.3, adjusted with NaOH. 0.5-ml aliquots of the suspension were used for measurement of fluorescence by a CAF 110 spectrophotometer (JASCO, Tokyo, Japan). CaCl₂ was added to the suspension at a final concentration of 2 mM immediately before measurement (normal Krebs-HEPES). For measurement of [Ca²⁺]_i, fura-2 was excited at two wavelengths of 340 nm and 380 nm, and emission was monitored at 500 nm at 25°C. [Ca²⁺]_i values were calculated from fura-2 fluorescence ratios (R) according to the following equation:

$$[Ca^{2+}]_i = Kd(S_{12}/S_{b2}(R - R_{min})/(R_{max} - R))$$

where R_{max} and R_{min} are the ratios, e.g., 340 nm/380 nm, obtained at saturating and zero Ca²⁺ concentrations by adding Triton X-100 and subsequently EGTA at final concentrations of 0.1% and 5 mM, respectively, Kd is defined as 224 nM, S_{b2} is the 380 nm excitation signal at the saturating Ca²⁺ concentration, and S₁₂ is the 380 nm excitation signal in the absence of Ca²⁺.

Electrophysiology

A7r5 cells were perfused with Krebs-HEPES solution containing 2 mM Ca²⁺, visualized with Nomarski optics (Carl-Zeiss Axioskop) and whole-cell recordings were made with thin-wall

borosilicate glass patch pipettes (resistance, 3–5 MΩ) as described previously (Enoki *et al.*, 1995b; Kobayashi & Takahashi, 1993; Minowa *et al.*, 1997). Pipettes were filled with Cs-aspartate solution containing (in mM): Cs-aspartate 120, CsCl 20, MgCl₂ 2, HEPES 10, EGTA 10 (pH 7.3, adjusted with CsOH). EGTA was added to the pipette solution at a final concentration of 10 mM, a concentration having enough buffering capacity for Ca²⁺ to prevent a transient increase in [Ca²⁺]_i (Neher, 1988), and the concentration of free Ca²⁺ in the solution was maintained at 100 nM by adding the amount of CaCl₂ as described by Van Heeswijk *et al.* (1984). Tight seal whole-cell currents were recorded with an EPC 7 patch-clamp amplifier (List, Darmstadt, Germany) and analysed with the pClamp software package (Axon Instruments, Burlingame, CA, U.S.A.). Perfusion rate was maintained at 2.2–2.5 ml min⁻¹ and the bath volume was ~1.0 ml. All experiments were done under voltage-clamp at a holding potential of -60 mV at room temperature (22–24°C). To examine the Ca²⁺ currents through the cation channel, the bath solution was switched from Krebs-HEPES to 30 mM Ca²⁺/100 mM N-methyl-D-glucamine (NMDG) solution which contained (in mM): CsCl₂ 30, NMDG chloride 100, MgCl₂ 1, glucose 11, HEPES 10 (pH 7.4, adjusted with Tris). In all experiments, the bath solution was supplemented with 1 μM nifedipine to block Ca²⁺ entry through VOC. Current-voltage relationships were obtained by applying voltage steps of 100 ms duration ranging from -100 to +80 mV in 20 mV increments before and after application of drugs. The drug-induced currents at each membrane potential were determined by subtracting currents before application of the drug from currents after its application.

Statistical analysis

All results were expressed as mean ± s.e.mean. The data were subjected to a two-way analysis of variance, and when a

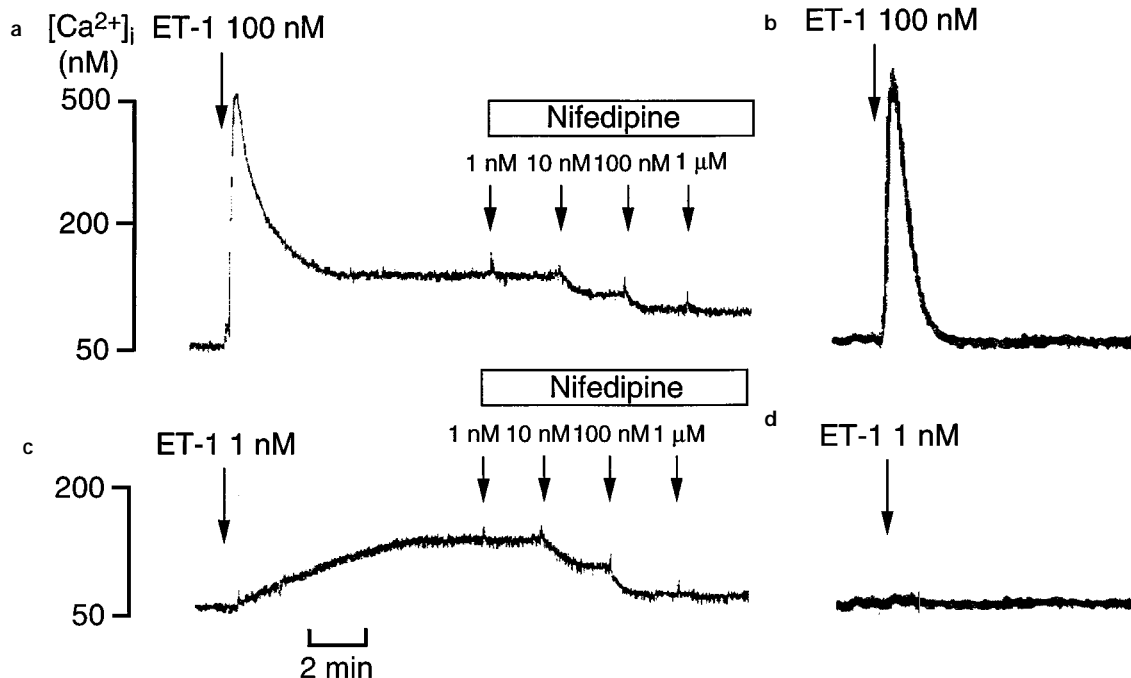


Figure 1 Effects of varying concentrations of nifedipine on elevations in intracellular free Ca²⁺ concentrations ([Ca²⁺]_i) induced by endothelin-1 (ET-1) in fura 2-loaded A7r5 cells. (a and c) Original tracings illustrating the pattern of elevations in [Ca²⁺]_i induced by a higher concentration (100 nM; a) or a lower concentration (1 nM; c) of ET-1 and the effects of varying concentrations of nifedipine on the elevations. (b and d) Original tracings illustrating the pattern of elevations in [Ca²⁺]_i induced by a higher concentration (100 nM; b) or a lower concentration (1 nM; d) of ET-1 in media lacking Ca²⁺.

significant *F* value was encountered, Newman-Keuls' multiple-range test was used to test for significant differences between treatment means. A probability level of *P*<0.05 was considered statistically significant.

Drugs

Chemicals were obtained from the following sources: ET-1, from Peptide Institute (Osaka, Japan); fura-2/AM and EGTA, from Dojindo Laboratories (Kumamoto, Japan); nifedipine, from Sigma (St. Louis, MO, U.S.A.); SK&F 96365, from Biomol (Plymouth Meeting, PA, U.S.A.). Nifedipine was dissolved in ethanol and the final concentration of ethanol was lower than 0.1%.

Results

[Ca²⁺]_i measurement in A7r5 cells

In resting A7r5 cells, [Ca²⁺]_i was 54±16 nM, mean±s.e. (*n*=30). As shown in Figure 1a, a higher concentration (100 nM) of ET-1 evoked biphasic changes in [Ca²⁺]_i in A7r5 cells consisting of an initial transient peak and a subsequent sustained phase: the values were 450±88 (*n*=5) and 143±40 nM (*n*=5), respectively. ET-1 at 10 nM also induced biphasic changes in [Ca²⁺]_i but the transient phase was smaller (245±79 nM, *n*=5; *P*<0.01, significantly different from the value at 100 nM ET-1) with the sustained phase being unchanged (124±37 nM, *n*=5). In contrast, a lower concen-

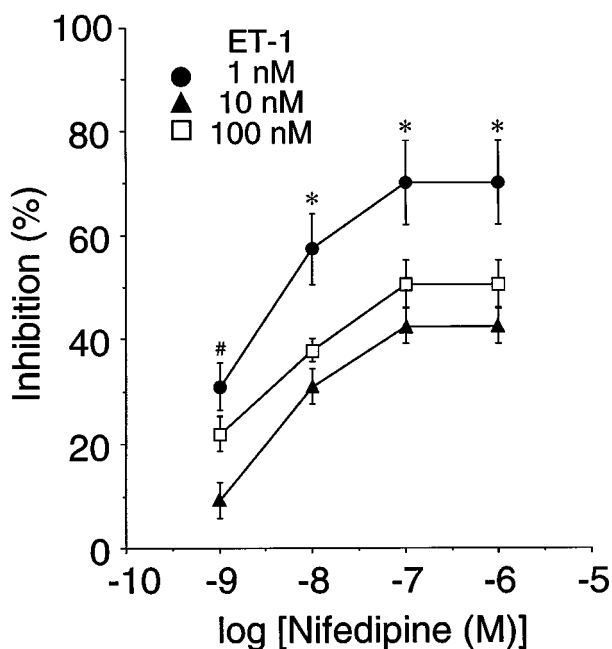


Figure 2 The concentration-response relationships for inhibition by nifedipine of the elevations in [Ca²⁺]_i induced by 1 nM, 10 nM and 100 nM ET-1. The extent of the inhibition was represented by a percentage of the value just before addition of nifedipine. Each point represents mean values±s.e.mean of five experiments. **P*<0.01; #*P*<0.05: significantly different from the value at 10 nM and 100 nM ET-1.

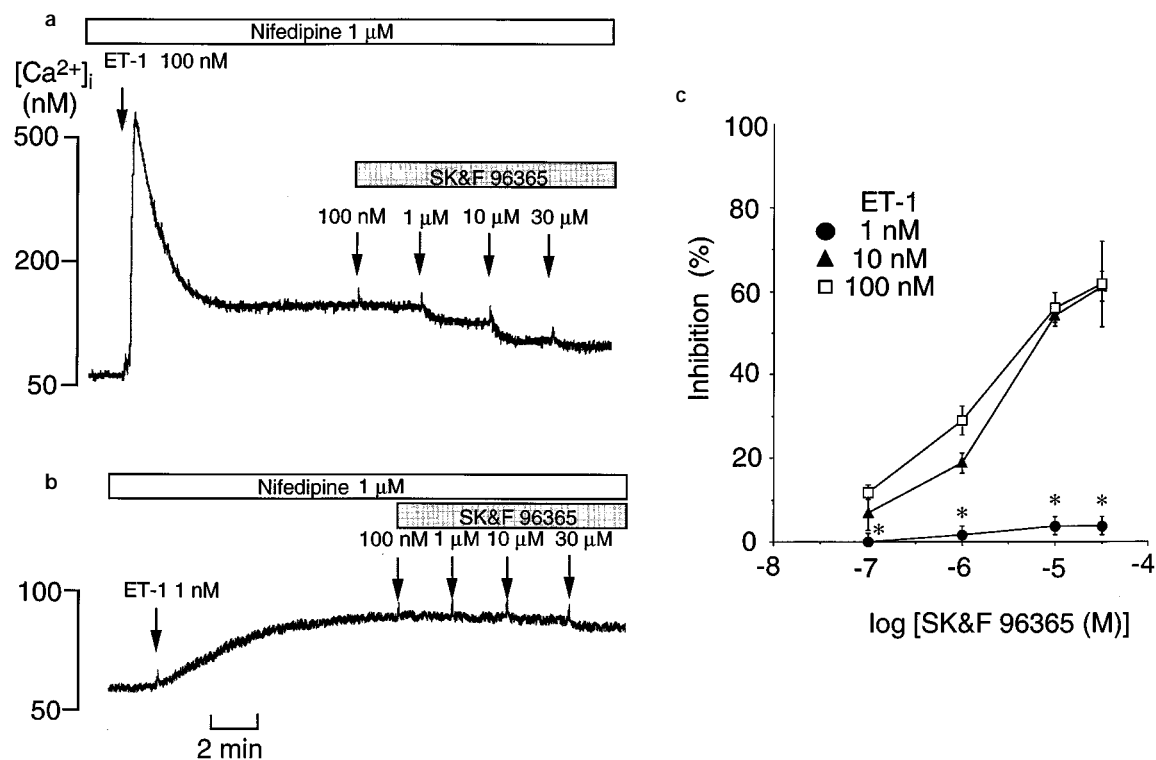


Figure 3 Effects of varying concentrations of SK&F 96365 on elevations in intracellular free Ca²⁺ concentrations ([Ca²⁺]_i) induced by endothelin-1 (ET-1) in fura 2-loaded A7r5 cells in the presence of 1 μM nifedipine. (a and b) Original tracings illustrating the effects of varying concentrations of SK&F 96365 on elevations in [Ca²⁺]_i induced by a higher concentration (100 nM; a) or a lower concentration (1 nM; b) of ET-1. (c) The concentration-response relationships for inhibition by SK&F 96365 of the elevations in [Ca²⁺]_i induced by 1 nM, 10 nM, and 100 nM ET-1 in the presence of 1 μM nifedipine. The extent of the inhibition was represented by a percentage of the value just before addition of SK&F 96365. Each point represents mean values±s.e.mean of six experiments. **P*<0.01; significantly different from the value at 10 nM and 100 nM ET-1.

tration (1 nM) of ET-1 evoked only a sustained elevation where $[\text{Ca}^{2+}]_i$ was 101 ± 27 nM ($n=5$) (Figure 1b).

A specific blocker of L-type VOC nifedipine suppressed the sustained elevation in $[\text{Ca}^{2+}]_i$ induced by 100 nM ET-1 in a concentration-dependent manner, and its effect reached the maximal level at $1 \mu\text{M}$ where the inhibition amounted to $50.2 \pm 7.4\%$ ($n=5$) (Figures 1a and 2).

Essentially similar results were obtained by use of 10 nM ET-1 (Figure 2): the inhibition by $1 \mu\text{M}$ nifedipine was $43.8 \pm 5.8\%$ ($n=5$). Notably, when $1 \mu\text{M}$ ET-1 was used instead of 10 nM or 100 nM, the inhibitory effect of nifedipine was more marked: the inhibition amounted to $70.5 \pm 11.4\%$ ($n=5$, significantly different from the value at 10 nM or 100 nM ET-1) (Figures 1c and 2).

The sustained phase induced by lower or higher concentrations of ET-1 was abolished after removal of extracellular Ca^{2+} (Figure 1b and d), indicating that the sustained phase results mainly from transmembrane Ca^{2+} influx.

To determine what types of Ca^{2+} entry channel are involved in the nifedipine-resistant part of the sustained elevation in $[\text{Ca}^{2+}]_i$ induced by ET-1, we examined the effects of SK&F 96365 in the presence of $1 \mu\text{M}$ nifedipine to completely block VOC.

In the presence of $1 \mu\text{M}$ nifedipine, the $[\text{Ca}^{2+}]_i$ in resting A7r5 cells was 56 ± 14 nM ($n=25$) which was not significantly different from the value in the absence of nifedipine. Under this condition, 100 nM ET-1 also evoked biphasic changes in $[\text{Ca}^{2+}]_i$ in A7r5 cells with the initial transient peak of 380 ± 140 nM ($n=6$) and the sustained phase of 123 ± 50 nM ($n=6$). SK&F 96365 suppressed the nifedipine-resistant part of the sustained elevation in $[\text{Ca}^{2+}]_i$ induced by 100 nM ET-1 in a concentration-dependent manner, and the maximum inhibition was observed at concentrations higher than $10 \mu\text{M}$: the inhibition by $10 \mu\text{M}$ SK&F 96365 amounted to $59.9 \pm 12.6\%$ ($n=6$) (Figure 3a and d). When 10 nM ET-1 was used,

essentially similar results were obtained (Figure 3c): the inhibition by $10 \mu\text{M}$ SK&F 96365 was $59.7 \pm 3.8\%$ ($n=6$). In contrast, totally different results were obtained, when a lower concentration (1 nM) of ET-1 was used (Figure 3b and c): in this case, SK&F 96365 up to the concentration of $30 \mu\text{M}$ had no significant effect on the nifedipine-resistant part of the sustained elevation in $[\text{Ca}^{2+}]_i$: the inhibition by SK&F 96365 was $2.9 \pm 1.9\%$ ($n=6$).

Based on the sensitivities to nifedipine and SK&F 96365, the sustained elevation in $[\text{Ca}^{2+}]_i$ can be divided into two groups. The elevation induced by lower concentrations (≤ 1 nM) of ET-1 is a resistant to SK&F 96365 but more sensitive to nifedipine, whereas the elevation induced by higher concentrations (≥ 10 nM) of ET-1 is sensitive to SK&F 96365 but less sensitive to nifedipine.

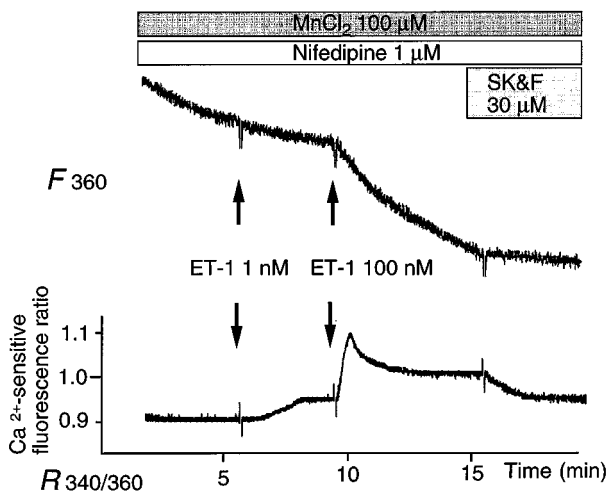


Figure 4 Original tracings illustrating the effects of a lower (1 nM) or a higher concentration (100 nM) of ET-1 on Mn^{2+} -quenching of fura-2 fluorescence in A7r5 cells in the presence of $1 \mu\text{M}$ nifedipine and their modification by SK&F 96365. At the beginning of experiments, MnCl_2 and nifedipine were added to incubation medium at a final concentration of $100 \mu\text{M}$ and $1 \mu\text{M}$, respectively, and fluorescence was monitored with an excitation wavelength at 360 nm and an emission wavelength at 500 nm for Mn^{2+} -quenching. ET-1 at 1 nM or 100 nM and SK&F 96365 at $30 \mu\text{M}$ were added at the time indicated by arrows and a bar, respectively. For reference, changes in $[\text{Ca}^{2+}]_i$ were simultaneously measured by monitoring the fura-2 fluorescence at excitation wavelengths of 340 nm and 360 nm and an emission wavelength of 500 nm.

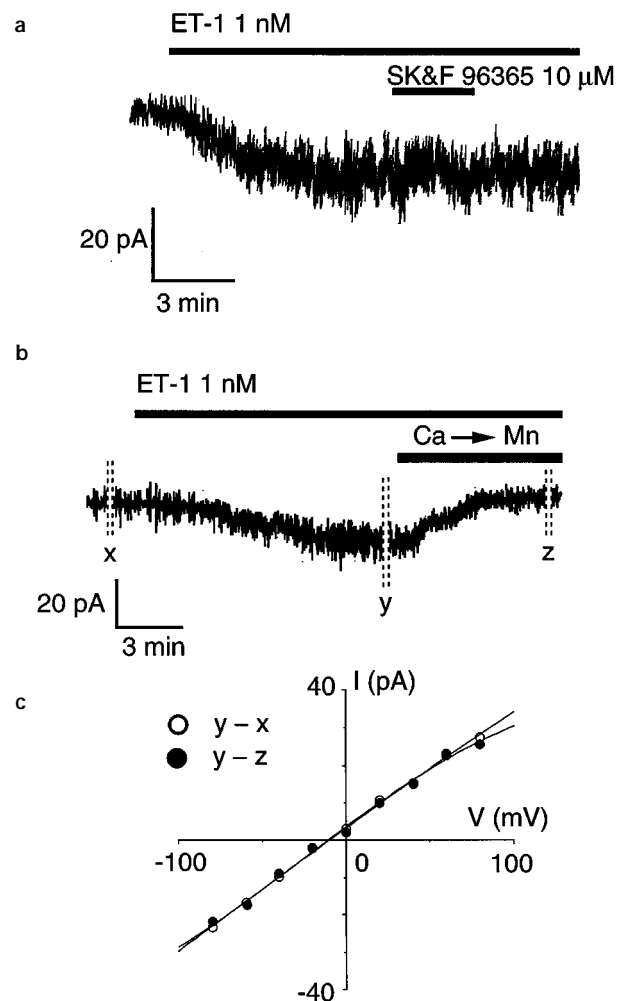


Figure 5 Whole-cell recordings of inward currents induced by a lower concentration (1 nM) of ET-1 in A7r5 cells in the presence of $1 \mu\text{M}$ nifedipine. The cells were clamped at a holding potential of -60 mV with the whole-cell configuration and ET-1 was added to the bath solution at a final concentration of 1 nM during the time interval indicated by a horizontal bar. After the ET-1 induced currents had reached a steady-state, SK&F 96365 was added to the bath solution at a final concentration of $10 \mu\text{M}$ (a) or Ca^{2+} in the bath solution was replaced by 2 mM Mn^{2+} (b). (c) The current-voltage relationships for the ET-1-induced current and the current inhibited by replacement of Ca^{2+} with Mn^{2+} . At the time indicated by x, y and z in panel b, voltage steps of 100-ms duration ranging from -100 to $+80$ mV in 20-mV increments were applied. The currents induced by ET-1 were obtained by subtracting currents at x from those at y, and the currents inhibited by replacement of Ca^{2+} with Mn^{2+} were obtained by subtracting currents at z from those at y.

To further characterize the properties of the sustained elevation in [Ca²⁺]_i induced by ET-1, we examined Mn²⁺ quenching of the fura-2 fluorescence as an index of Mn²⁺ entry. In the presence of 1 μM nifedipine, exposure of the cells to 1 nM ET-1 had little effect on the rate of quenching of fura-2 fluorescence which was excited at 360 nm and monitored at 500 nm (Figure 4). In contrast, exposure of the cells to 100 nM ET-1 induced a marked increase of the quenching rate, which was blocked by 30 μM SK&F 96365.

Whole-cell current in A7r5 cells

To further elucidate the characteristics of the Ca²⁺ entry, whole-cell recordings were performed with A7r5 cells. At a holding potential of -60 mV, addition of ET-1 to the bath solution at concentrations from 100 pM to 10 nM induced a slow inward current with an increase in baseline 'noise' (Figures 5 and 6).

The current induced by a lower concentration (1 nM) of ET-1 showed a linear current-voltage relationship against the membrane potential between -100 mV and +80 mV with the reversal potential of -15.6 ± 12.5 mV (*n* = 11) (Figure 5c). In most cells, the responses continued for over 30 min after washout of ET-1. The current was totally resistant to 10 μM SK&F 96365 (Figures 5a and 7), but it was abolished when Ca²⁺ in the bath solution was replaced by 2 mM Mn²⁺ (Figures 5b and 7). The characteristics of the current inhibited by the replacement were essentially similar to the ET-1-induced current in terms of the linear current-voltage relationship and the reversal potential.

The current induced by a higher concentration (10 nM) of ET-1 also showed a linear current-voltage relationship against the membrane potential with the reversal potential of -14.7 ± 3.7 mV (*n* = 18) (Figure 6a). In most cells, the responses also continued for over 30 min after washout of ET-1. Notably, the current was partially sensitive to 10 μM SK&F 96365 and the inhibitory effect of the drug was reversible (Figures 6a and 7). The characteristics of the current inhibited by SK&F 96365 were essentially similar to the ET-1 induced current, in terms of the linear current-voltage relationship and the reversal potential.

As shown in Figures 6b and 7, the ET-1-induced current was partially suppressed after replacement of Ca²⁺ in the bath solution by 2 mM Mn²⁺ (33.3 ± 9.2%, *n* = 4). When 10 μM SK&F 96365 was added to the bath solution after the replacement, the ET-1-induced current was completely suppressed (Figures 6b and 7). Again, the characteristics of the current inhibited by SK&F 96365 were essentially similar to the ET-1-induced current, in terms of the linear current-voltage relationship and the reversal potential.

In the presence of 10 μM SK&F 96365, 10 nM ET-1 induced a current with a linear current-voltage relationship and the reversal potential of -15.3 ± 5.2 mV (*n* = 3) (Figure 6c). When Ca²⁺ in the bath solution was replaced by 2 mM Mn²⁺ in the presence of 10 μM SK&F 96365, the ET-1-induced current was completely suppressed (Figure 6c).

Figure 7 summarizes the effect of 10 μM SK&F 96365, replacement of Ca²⁺ in the bath solution by 2 mM Mn²⁺ or their combination on the currents induced by 100 pM, 1 nM and 10 nM ET-1. The currents induced by lower concentra-

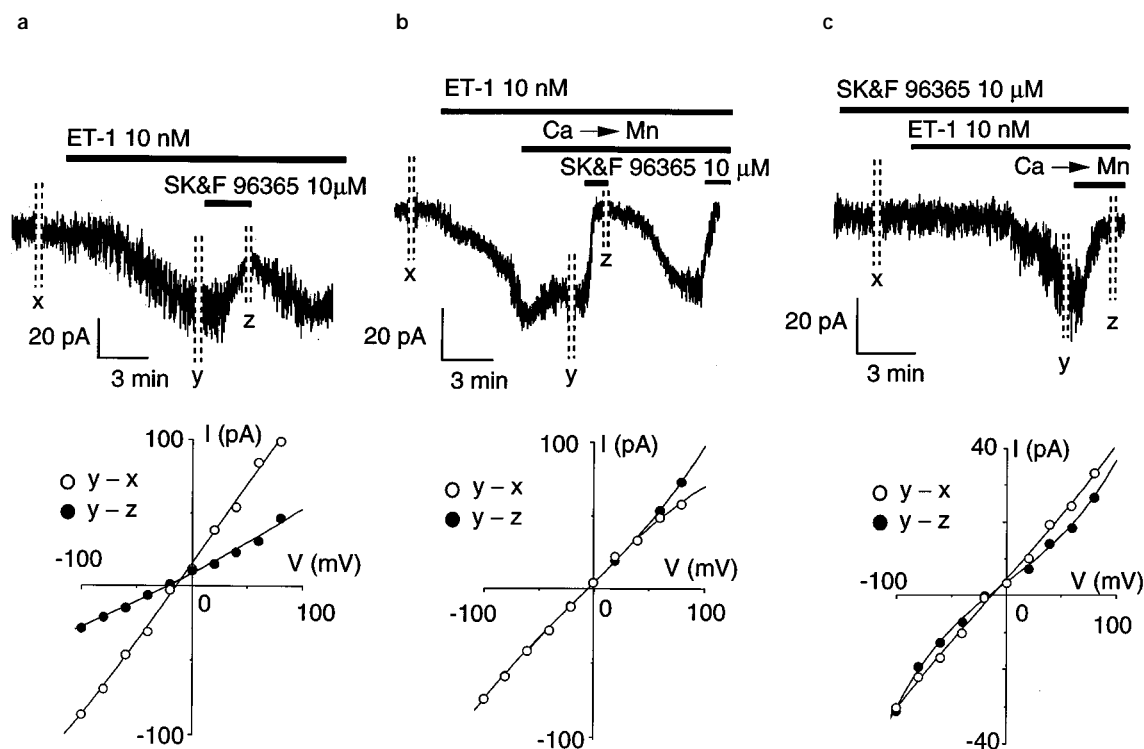


Figure 6 Effects of SK&F 96365, replacement of Ca²⁺ with Mn²⁺ in the bath solution or their combination on whole-cell currents induced by a higher concentration (10 nM) of ET-1 in A7r5 cells in the presence of 1 μM nifedipine. The cells were clamped at a holding potential of -60 mV with the whole-cell configuration. Upper and lower panels show typical tracings of whole-cell recordings and current-voltage relationships, respectively. ET-1 or SK&F 96365 was added to the bath solution at a final concentration of 10 nM or 10 μM, respectively, during the time intervals indicated by horizontal bars. In (b) and (c), Ca²⁺ in the bath solution was replaced by 2 mM Mn²⁺ (indicated by Ca → Mn). At the time indicated by x, y and z in each panel, voltage steps ranging from -100 to +80 mV in 20-mV increments were applied. The currents induced by ET-1 were obtained by subtracting currents at x from those at y, and the currents inhibited by SK&F 96365 or replacement of Ca²⁺ with Mn²⁺ were obtained by subtracting currents at z from those at y.

tions (100 pM and 1 nM) of ET-1 were resistant to SK&F 96365, but they were abolished by replacement of Ca^{2+} in the bath solution with 2 mM Mn^{2+} . In contrast, the current induced by a higher concentration (10 nM) of ET-1 was highly sensitive to 10 μM SK&F 96365 but less sensitive to replacement of Ca^{2+} in the bath solution by 2 mM Mn^{2+} : the inhibition by these treatments were $54.8 \pm 6.9\%$, ($n=5$) and $33.3 \pm 9.2\%$ ($n=5$), respectively. In addition, the currents induced by 10 nM ET-1 were abolished by combined treatment with 10 μM SK&F 96365 and replacement of Ca^{2+} in the bath solution by 2 mM Mn^{2+} ($95.9 \pm 7.0\%$, $n=4$).

Finally we examined the Ca^{2+} currents activated by ET-1. For this purpose, all the cations in the bath solution were replaced by 30 mM Ca^{2+} and nonpermeant cation NMDG. Even after this replacement, ET-1 at 1 nM evoked an inward current (Figure 8a), which was abolished by adding 2 mM Mn^{2+} to the bath solution (Figure 8a). ET-1 at 10 nM also evoked an inward current in the same bath solution, which was partially and reversibly blocked by 10 μM SK&F 96365 (Figure 8b).

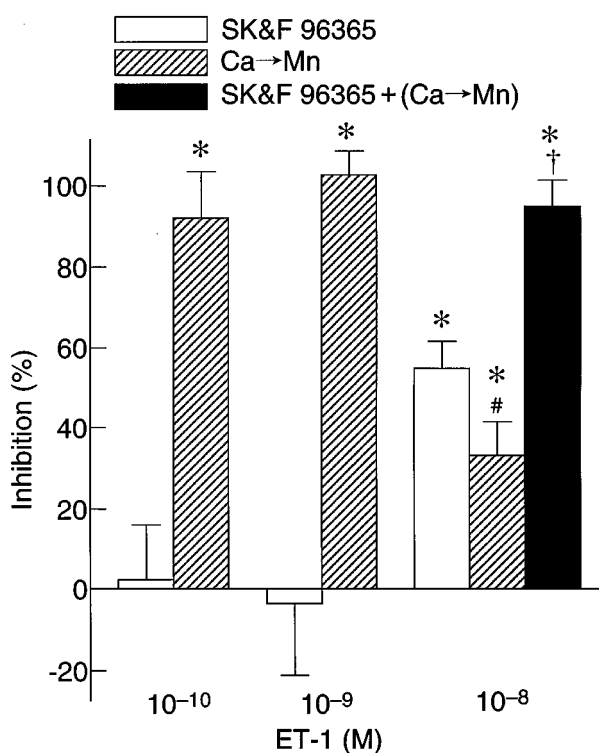


Figure 7 Summary of the inhibitory effects of 10 μM SK&F 96365, replacement of Ca^{2+} in the bath solution by 2 mM Mn^{2+} or their combination on whole-cell inward currents induced by varying concentrations (100 pM, 1 nM and 10 nM) of ET-1 in A7r5 cells in the presence of 1 μM nifedipine. A7r5 cells were clamped at a holding potential of -60 mV with the whole-cell configuration. After the ET-1-induced currents had reached a steady-state, 10 μM SK&F 96365 was added to the bath solution (open bars) or Ca^{2+} in the bath solution was replaced by 2 mM Mn^{2+} (hatched bars). In some experiments (rightmost bar), SK&F 96365 was added after Ca^{2+} in the bath solution had been replaced by 2 mM Mn^{2+} . The inhibition was represented by a percentage of the suppressed current to the current just before addition of SK&F 96365 or replacement of Ca^{2+} by 2 mM Mn^{2+} . Each bar represents mean values \pm s.e. mean of 7, 4, 6, 5, 5, 3 or 4 experiments (from leftmost bar). * $P < 0.01$; significantly different from the currents before the treatment. # $P < 0.01$; significantly different from the inhibition by replacement with Mn^{2+} at 100 pM and 1 nM ET-1. $\ddagger P < 0.01$; significantly different from the inhibition by either SK&F 96365 or replacement with Mn^{2+} at 10 nM ET-1.

Discussion

Measurement of $[\text{Ca}^{2+}]_i$ in A7r5 cells

In the present study using A7r5 cells, higher concentrations (≥ 10 nM) of ET-1 evoked an increase in $[\text{Ca}^{2+}]_i$ consisting of two components: a rapid initial transient phase and a sustained phase (Figure 1a). In contrast, lower concentrations (≤ 1 nM) of ET-1 induced only a sustained phase (Figure 1c). The sustained phase induced by both concentrations of ET-1 was totally abolished by removal of extracellular Ca^{2+} (Figure 1b and d). These results are consistent with previous results (Enoki *et al.*, 1995a,b; Minowa *et al.*, 1997) and indicate that the sustained phase is due to transmembrane Ca^{2+} influx, whereas the initial transient phase is the result of mobilization of Ca^{2+} from intracellular stores via increased formation of IP_3 , as noted previously (Kasuya *et al.*, 1989; Van Renterghem *et al.*, 1988). Conversely, these data suggest that Ca^{2+} signaling of ET-1 is different depending on its concentrations; higher concentrations of ET-1 induces activation of Ca^{2+} entry channel with increased formation of IP_3 , whereas lower concentrations of ET-1 exclusively activate Ca^{2+} entry channel.

The sustained increase in $[\text{Ca}^{2+}]_i$ was partially sensitive to an inhibitor of L-type VOC nifedipine. This result is consistent with previous reports (Goto *et al.*, 1989; Inoue *et al.*, 1990) and indicates that this part of the increase is the result of Ca^{2+} influx through VOC. However, the sensitivity to nifedipine was different depending on the concentrations of ET-1: about half of the increase induced by higher concentrations of ET-1 was eliminated by nifedipine, whereas about 70% of the increase induced by lower concentrations of ET-1 was eliminated (Figures 1 and 2).

The nifedipine-resistant part of the sustained increase in $[\text{Ca}^{2+}]_i$ induced by lower concentrations of ET-1 was totally insensitive to a maximally effective concentration (≥ 10 μM) of an inhibitor of voltage-independent Ca^{2+} channel SK&F 96365 (Figure 3b). In contrast, the nifedipine-resistant increase in $[\text{Ca}^{2+}]_i$ induced by higher concentrations of ET-1 was partially sensitive to SK&F 96365, although the remaining part was insensitive to this blocker (Figure 3a and c). These results show that at lower concentrations of ET-1, only SK&F 96365-resistant Ca^{2+} entry channel is activated, whereas SK&F 96365-sensitive Ca^{2+} entry channel becomes activated with increases in the concentrations of ET-1 in addition to the former channel. Furthermore, these data also show that at all concentrations of ET-1, VOC is activated.

Stimulation of the cells by higher concentrations of ET-1 induced an increase in the rate of Mn^{2+} quenching of fura-2 fluorescence, which was blocked by SK&F 96365. In contrast, stimulation by lower concentrations of ET-1 was without effect on the rate (Figure 4). These results show that Ca^{2+} entry channel activated by lower concentrations of ET-1 is impermeable to Mn^{2+} , whereas the channel activated by higher concentrations of ET-1 is permeable to Mn^{2+} .

Whole-cell current recordings

The current induced by lower concentrations ET-1 (≤ 1 nM) The characteristics of the current induced by lower concentrations of ET-1 (the linear current-voltage relationship and its reversal potential close to 0 mV) indicate that the channel is either equally permeable to both extracellular Na^+ and intracellular Cs^+ (Figure 5) or only to Cl^- . The latter possibility can be excluded because the calculated equilibrium potential for Cl^- (E_{Cl^-} ; -46.9 mV in normal Krebs-HEPES

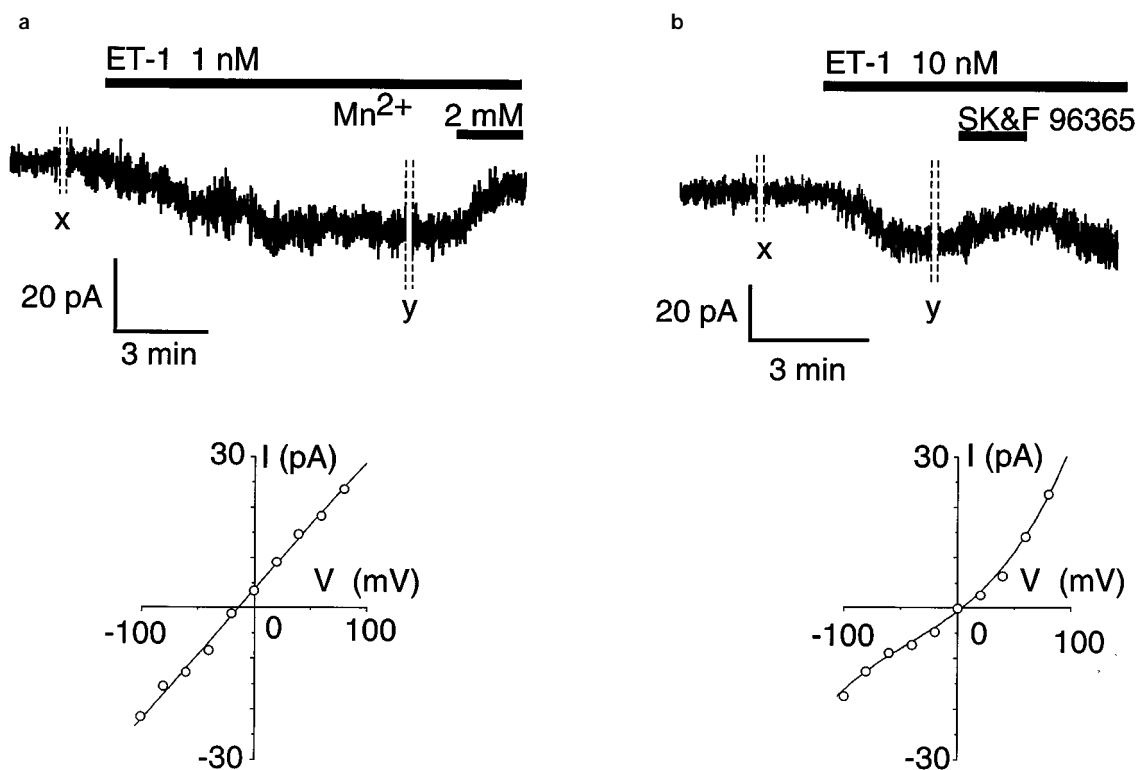


Figure 8 Whole-cell recordings of inward currents induced by ET-1 in A7r5 cells in the presence of 1 μM nifedipine in 30 mM Ca²⁺ 100 mM N-methyl-D-glucamine (NMDG) solution in A7r5 cells. The cells were clamped at a holding potential of -60 mV with the whole-cell configuration. Upper and lower panels show typical tracings of whole-cell recordings and current-voltage relationships, respectively. ET-1 was added to the bath solution at a final concentration of 1 nM (a) or 10 nM (b) during the time interval indicated by a horizontal bar. After the ET-1-induced current had reached a steady-state, MnCl₂ (a) or SK&F 96365 (b) was added to the bath solution at a final concentration of 2 mM and 10 μM , respectively. At the time indicated by x and y, voltage steps ranging from -100 to $+80$ mV in 20-mV increments were applied and the current induced by ET-1 was obtained by subtracting currents at x from those at y.

solution) is not close to the reversal potential, and because the pipette solution contains excess EGTA to completely suppress the increase in $[\text{Ca}^{2+}]_i$ which might trigger Ca²⁺-activated Cl⁻ current. Thus it can be concluded that the channel activated by low concentrations of ET-1 is nonselective cation channel.

The current was resistant to SK&F 96365 (Figures 5a and 7) and impermeable (or very low permeability) to Mn²⁺ (Figure 4). Notably the current was completely blocked when Ca²⁺ in the bath solution was replaced by Mn²⁺ (Figures 5b and 7). Most importantly, this channel was permeable to Ca²⁺, based on the data that the current was induced even in the medium containing only Ca²⁺ as a movable cation (Figure 8a). This channel seems to be different from SOCC, because increased formation of IP₃ and subsequent Ca²⁺ mobilization from internal stores are absent at these concentrations of ET-1 (Figures 1, 3 and 4) and because it is resistant to SK&F 96365 which is reported to block SOCC (Chung *et al.*, 1994; Franzius *et al.*, 1994; Koch *et al.*, 1994; Wayman *et al.*, 1996).

It is likely that this channel is responsible for the sustained increase in $[\text{Ca}^{2+}]_i$ induced by lower concentrations of ET-1, judging from the impermeability to Mn²⁺ and insensitivity to SK&F 96365. In terms of these properties, this channel seems to be an as yet unidentified Ca²⁺-permeable nonselective cation channel.

The current induced by higher concentrations of ET-1 (≥ 10 nM) In contrast, the current induced by higher concentrations of ET-1 (≥ 10 nM) was sensitive to both SK&F

96365 and replacement of Ca²⁺ in the bath solutions by 2 mM Mn²⁺ and the sum of their percentage inhibitions adds up to about 100% (Figures 6 and 7). These data indicate that the current induced by higher concentrations of ET-1 (≥ 10 nM) can be divided into two components based on the sensitivity to SK&F 96365 and permeability to Mn²⁺. One component is resistant to SK&F 96365 and impermeable to Mn²⁺ (Figure 6a, c and 7). In this sense, this channel is considered to be the same channel as that activated by lower concentrations of ET-1.

The other component which is activated specifically by higher concentrations of ET-1 is sensitive to SK&F 96365 and permeable to Mn²⁺ (Figures 6a, b and 7). This current also seems to be conducted through nonselective cation channel based on the following observations. First, the total current induced by higher concentrations of ET-1 showed the linear current-voltage relationship and the reversal potential close to 0 mV (Figure 6a), which was not different from the value obtained by lower concentrations of ET-1 (Figure 5). Secondly, the current inhibited by SK&F 96365 is characterized by the linear current-voltage relationship and the reversal potential close to 0 mV (Figure 6b).

The channel activated specifically by higher concentrations of ET-1 is also permeable to Ca²⁺. That is, the total Ca²⁺ current induced by higher concentrations of ET-1 consists of two components: SK&F 96365-sensitive and -insensitive components (Figure 8b). The SK&F 96365-insensitive component is considered to result from the channel activated by lower

concentrations of ET-1, judging from its sensitivity to Mn²⁺ and insensitivity to this drug (Figures 5 and 8). It follows that SK&F 96365-sensitive component of the Ca²⁺ current is specific for higher concentrations of ET-1. These data strongly indicate that Ca²⁺-permeable nonselective cation channel contributes mainly to the increase in [Ca²⁺]_i induced by higher concentrations of ET-1.

As described in Introduction, voltage-independent Ca²⁺ channels are usually classified into four groups according to the mode of activation. The nonselective cation channel activated by lower concentrations of ET-1 but not by higher concentrations is unlikely to be SOCC, because ET-1 at these concentrations does not stimulate formation of IP₃ (and hence store depletion) and because the channel is resistant to SK&F 96365 which is reported to block SOCC (Chung *et al.*, 1994; Franzius *et al.*, 1994; Koch *et al.*, 1994; Wayman *et al.*, 1996). Since it is well-known that stimulation of ET_A receptors causes increased formation of second messengers like cyclic AMP

(Aramori & Nakanishi 1992; Takagi *et al.*, 1995), it is possible that the channels are activated by second messengers (second-messenger-operated channels). Alternatively, the channels could be directly activated by G-proteins (G-protein-operated channels), considering that ET_A receptors are coupled with G-proteins (Rubanyi & Polokoff, 1994). The cellular mechanisms for activation of these two channels are now under investigation in our laboratory.

In summary, the present study demonstrate that in addition to VOC, stimulation by ET-1 can activate two types of Ca²⁺-permeable nonselective cation channel: lower concentrations of ET-1 activate Ca²⁺-permeable nonselective cation channel which is resistant to SK&F 96365 and impermeable to Mn²⁺, whereas higher concentrations of ET-1 activate another type of Ca²⁺-permeable nonselective cation channel which is sensitive to SK&F 96365 and permeable to Mn²⁺ in addition to the SK&F 96365-resistant channel.

References

- ARAMORI, I. & NAKANISHI, S. (1992). Coupling of two endothelin receptor subtypes to differing signal transduction in transfected Chinese hamster ovary cells. *J. Biol. Chem.*, **267**, 12468–12474.
- BENHAM, C.D. & TSIEN, R.W. (1987). A novel receptor-operated Ca²⁺-permeable channel activated by ATP in smooth muscle. *Nature*, **328**, 275–278.
- CHUNG, S.C., MCDONALD, T.V. & GARDNER, P. (1994). Inhibition by SK&F 96365 of Ca²⁺ current, IL-2 production and activation in T lymphocytes. *Br. J. Pharmacol.*, **113**, 861–868.
- CLEMENTI, E. & MELDOLESI, J. (1996). Pharmacological and functional properties of voltage-independent Ca²⁺ channels. *Cell Calcium*, **19**, 269–279.
- ENOKI, T., MIWA, S., SAKAMOTO, A., MINOWA, T., KOMURO, T., KOBAYASHI, S., NINOMIYA, H. & MASAKI, T. (1995a). Functional coupling of ET_A receptor with Ca²⁺-permeable nonselective cation channel in mouse fibroblasts and rabbit aortic smooth-muscle cells. *J. Cardiovasc. Pharmacol.*, **26**, S258–S261.
- ENOKI, T., MIWA, S., SAKAMOTO, A., MINOWA, T., KOMURO, T., KOBAYASHI, S., NINOMIYA, H. & MASAKI, T. (1995b). Long-lasting activation of cation current by low concentration of endothelin-1 in mouse fibroblasts and smooth muscle cells of rabbit aorta. *Br. J. Pharmacol.*, **115**, 479–485.
- FASOLATO, C., INNOCENTI, B. & POZZAN, T. (1994). Receptor-activated Ca²⁺ influx: how many mechanisms for how many channels? *Trends Pharmacol. Sci.*, **15**, 77–83.
- FELDER, C.C., SINGER-LAHAT, D. & MATHES, C. (1994). Voltage-independent calcium channels – Regulation by receptors and intracellular calcium stores. *Biochem. Pharmacol.*, **48**, 1997–2004.
- FRANZIUS, D., HOTH, M. & PENNER, R. (1994). Non-specific effects of calcium entry antagonists in mast cells. *Pflügers Arch.*, **428**, 433–438.
- GOTO, K., KASUYA, Y., MATSUKI, N., TAKUWA, Y., KURIHARA, H., ISHIKAWA, T., KIMURA, S., YANAGISAWA, M. & MASAKI, T. (1989). Endothelin activates the dihydropyridine-sensitive, voltage-dependent Ca²⁺ channel in vascular smooth muscle. *Proc. Natl. Acad. Sci. U.S.A.*, **86**, 3915–3918.
- GROSCHNER, K., GRAIER, W.F. & KUKOVETZ, W.R. (1994). Histamine induces K⁺, Ca²⁺, and Cl⁻ currents in human vascular endothelial cells. Role of ionic currents in stimulation of nitric oxide biosynthesis. *Circ. Res.*, **75**, 304–314.
- HOTH, M. & PENNER, R. (1992). Depletion of intracellular calcium stores activates a calcium current in mast cells. *Nature*, **355**, 353–358.
- HUANG, X.N., HISAYAMA, T. & TAKAYANAGI, I. (1990). Endothelin-1 induced contraction of rat aorta: contributions made by Ca²⁺ influx and activation of contractile apparatus associated with no change in cytoplasmic Ca²⁺ level. *Naunyn-Schmiedeberg's Arch. Pharmacol.*, **341**, 80–87.
- INOUE, Y., OIKE, M., NAKAO, K., KITAMURA, K. & KURIYAMA, H. (1990). Endothelin augments unitary calcium channel currents on the smooth muscle cell membrane of guinea-pig portal vein. *J. Physiol. Lond.*, **423**, 171–191.
- KASUYA, Y., TAKUWA, Y., YANAGISAWA, M., KIMURA, S., GOTO, K. & MASAKI, T. (1989). Endothelin-1 induces vasoconstriction through two functionally distinct pathways in porcine coronary artery: contribution of phosphoinositide turnover. *Biochem. Biophys. Res. Commun.*, **161**, 1049–1055.
- KOBAYASHI, S. & TAKAHASHI, T. (1993). Whole-cell properties of temperature-sensitive neurons in rat hypothalamic slices. *Proc. R. Soc. Lond. B.*, **251**, 89–94.
- KOCH, B.D., FAUROT, G.F., KOPANITSA, M.V. & SWINNEY, D. (1994). Pharmacology of a Ca²⁺-influx pathway activated by emptying the intracellular Ca²⁺ stores in HL-60 cells: evidence that a cytochrome P-450 is not involved. *Biochem. J.*, **302**, 187–190.
- KOMORI, S. & BOLTON, T.B. (1990). Role of G-proteins in muscarinic receptor inward and outward currents in rabbit jejunal smooth muscle. *J. Physiol.*, **427**, 395–419.
- MATTHEWS, G., NEHER, E. & PENNER, R. (1989). Second messenger-activated calcium influx in rat peritoneal mast cells. *J. Physiol.*, **418**, 105–130.
- MERRITT, J.E., ARMSTRONG, W.P., BENHAM, C.D., HALLAM, T.J., JACOB, R., JAXA-CHAMIEC, A., LEIGH, B.K., MCCARTHY, S.A., MOORES, K.E. & RINK, T.J. (1990). SK&F 96365, a novel inhibitor of receptor-mediated calcium entry. *Biochem. J.*, **271**, 515–522.
- MINOWA, T., MIWA, S., KOBAYASHI, S., ENOKI, T., ZHANG, X.-F., KOMURO, T., IWAMURO, Y. & MASAKI, T. (1997). Inhibitory effect of nitrovasodilators and cyclic GMP on ET-1-activated Ca²⁺-permeable nonselective cation channel in rat aortic smooth muscle cells. *Br. J. Pharmacol.*, **120**, 1536–1544.
- NEHER, E. (1988). The influence of intracellular calcium concentration on degranulation of dialysed mast cells from rat peritoneum. *J. Physiol. Lond.*, **395**, 193–214.
- RUBANYI, G.M. & POLOKOFF, M.A. (1994). Endothelins: molecular biology, biochemistry, pharmacology, physiology, and pathophysiology. *Pharmacol. Rev.*, **46**, 325–415.
- SIMPSON, A.W., STAMPFL, A. & ASHLEY, C.C. (1990). Evidence for receptor-mediated bivalent-cation entry in A10 vascular smooth-muscle cells. *Biochem. J.*, **267**, 277–280.
- TAKAGI, Y., NINOMIYA, H., SAKAMOTO, A., MIWA, S. & MASAKI, T. (1995). Structural basis of G protein specificity of human endothelin receptors. A study with endothelinA/B chimeras. *J. Biol. Chem.*, **270**, 10072–10078.
- VAN HEESWIJK, M.P., GEERTSEN, J.A. & VAN OS, C.H. (1984). Kinetic properties of the ATP-dependent Ca²⁺ pump and the Na⁺/Ca²⁺ exchange system in basolateral membranes from rat kidney cortex. *J. Membr. Biol.*, **79**, 19–31.
- VAN RENTERGHEM, C., VIGNE, P., BARHANIN, J., SCHMID ALLIANA, A., FRELIN, C. & LAZDUNSKI, M. (1988). Molecular mechanism of action of the vasoconstrictor peptide endothelin. *Biochem. Biophys. Res. Commun.*, **157**, 977–985.

WAYMAN, C.P., MCFADZEAN, I., GIBSON, A. & TUCKER, J.F. (1996). Two distinct membrane currents activated by cyclopiazonic acid-induced calcium store depletion in single smooth muscle cells of the mouse anococcygeus. *Br. J. Pharmacol.*, **117**, 566–572.

YANAGISAWA, M., KURIHARA, H., KIMURA, S., TOMOBE, Y., KOBAYASHI, M., MITSUI, Y., YAZAKI, Y., GOTO, K. & MASAKI, T. (1988). A novel potent vasoconstrictor peptide produced by vascular endothelial cells. *Nature*, **332**, 411–415.

(Received February 11, 1998

Revised March 24, 1998

Accepted May 12, 1998)